OBSERVATIONS OF BEAM LOSS PROTON TRAJECTORIES IN J-PARC LINAC*

H. Sako#, T. Maruta, and A. Miura, Japan Atomic Energy Agency, Tokai, Japan

Abstract

In J-PARC linac, highest beam loss has been observed in the ACS section at the H^- beam energy of 181 MeV. The primary source of the loss is considered to be H^0's produced by the electron stripping of H^-'s by the remnant gas inside the beam duct. The H^0 almost conserves the momentum of the H^- at the point where it has been produced, and almost 100% of the H^0's are converted into H^+'s (protons) through the beam duct. The H^+'s are expected to have small angles around 5 degrees with respect to the beam, with energies 100-150 MeV, according to a simulation. To detect H^+'s, we developed six-plane scintillating fiber detectors. The 2 planes are located at an upstream position and the other 4 planes are located about 1.1 m downstream of the beam. We measure each PMT signal by defining a trigger signal by coincidence of dynode signals of the most upstream and the most downstream PMT's.

We present preliminary results of time-of-flight measurements of charged particle tracks consistent with protons, and distributions of tracks along the beam axis.

INTRODUCTION

The H^0 ion produced by a beam H^- interacted with a remnant gas atom is considered to be the main source of the beam loss in the J-PARC ACS section. The primary aim of the present work is to identify H^+'s converted from H^0's when passing through the beam duct. For this purpose, we constructed six scintillating fiber detector planes. Each plane consists of 16 4 x 4 x 64 mm^3 plastic scintillating fibers. Each pair of planes are connected to a multi-anode photo-multipliers (PMT's) Hamamatsu H8500C. This pairing is to reduce inefficiency when a charged particle passes through a boundary between adjacent fibers in a plane.

Charged particle tracks are reconstructed with the fiber scintillating detector planes. Energy of each track is measured with the time-of-flight method in 1.1 m distance, and energy loss in each plane is also measured by light signal amplitude in a PMT to identify protons and reject other particle species such as electrons, X/gamma rays, and neutrons.

Another aim of this research is to measure beam loss source positions along the beam duct and identify hot spots, by projecting each track to the beam axis.

We have measured beam loss with fiber scintillator fiber detectors in ACS section at J-PARC linac since 2010 [1,2]. We already observed charged particle tracks successfully due to beam loss. Detailed description of the scintillating fiber counters and data acquisition system, see [1,2]. Since 2012, we use additional two fiber planes to measure vertical positions, and in total we use two upstream horizontal-measuring planes (H0, H1), two downstream horizontal-measuring planes (H2, H3) 1130 mm apart from H0/H1, and downstream vertical-measuring planes (V0, V1) 58 mm apart from H2/H3. In 2012 measurements, we changed signal cables from LAN cables to coaxial cables, which resulted in good signal shapes without satellite tails. The trigger signal was also improved as follows. Until 2011, we used a scheduled timing of the macro pulse as the start signal for TDC (Time-to-Digital Converter) CAEN V785 and the gate signal for QDC (charge (Q)-to-Digital Converter) CAEN V792. There were two serious problems. First, since the TDC has no multi-hit recording function, if there is another hit before relevant signal, a wrong combination of timings in fibers is recorded, and thus signal-to-background (S/N) ratio is significantly deteriorated. To solve this problem, we utilized final-stage dynode signals (DY) which are available for the PMT H8500C. The DY signals are opposite polarity (positive) signals to the negative anode signals. Since the PMT is a multi-anode PMT, the DY signal served as analog sum signal over all anode channels. We discriminate the DY signals of the three PMT's (DY1 for H0/H1, DY2 for H2/H3, and DY3 for V0/V1), and form coincidence signal of discriminated DY1 and DY3 for the start timing of TDC's and the timing gate of QDC's. The DY1 and DY3 coincidence signal (DY1&DY2) is used as a trigger of a charged particle track penetrating from H0 to V1. Timing and charge of individual anode signal can be measured with low accidental background by narrowing the duration between the start timing and the signal for TDC's, and the gate width for QDC's. We also formed a time gate (TG) from the scheduled beam start timing to define the timing within the macro pulse. The coincidence DY1&DY3&TG is used for the data taking. The timing offset and time interval per TDC channel for each fiber was calibrated by injecting a pulse generator signal split to all the detector signal cables end and measuring the timing with the data acquisition system.

RESULTS

The analysis shown here is based on the data taken from Apr. 2012 to Jun. 2012. The fiber geometry for H0, H1, H2, H3 is shown in Fig. 1. We have moved H2 and H3 to cover three different track angles through H0-H3 with respect to the beam axis. The angle acceptance is 3.6^o-5.0^o, 6.0^o-7.0^o, and 9.0^o-11.0^o.

*Work supported by JSPS KAKENHI Grant Numbers 23656063, 24510134.

#hiroyuki.sako@j-parc.jp

With TDC hits, we reconstruct a 3-dimensional track with the horizontal position of the fiber x^{hit}_i, the hit timing t^{hit}_i, and the position along beam axis z_i (upstream is the positive direction) at Plane Hi (i=0, 1, 2, 3). We require TDC hits in all 4 planes in H0-H3, and apply straight line fits as the following formulae in z-x, and z-t plane simultaneously;

$$x^{track} = X_0 + X_1 z^{track}$$
$$t^{track} = T_0 + T_1 z^{track} \quad ,$$

where X_0, X_1, T_0, T_1 are the fit parameters. In Fig. 2, the time residual t^{hit}_1- t^{track}_1 is plotted, where t^{track}_1 is t^{track} at $z=z_1$ (H1). A sharp signal peak for charged tracks with very low background is observed. The width from Gaussian fit is 0.40 nsec in r.m.s.

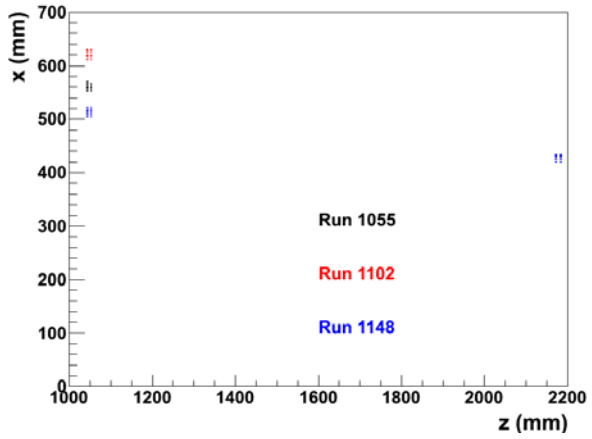

Figure 1: Fiber geometry is shown as a function of the z-position (mm) along the beam axis and the horizontal x-position (mm). The upstream fiber positions (z around 2170 mm) are common, while there are three configurations for downstream fiber positions (z around 1050 mm).

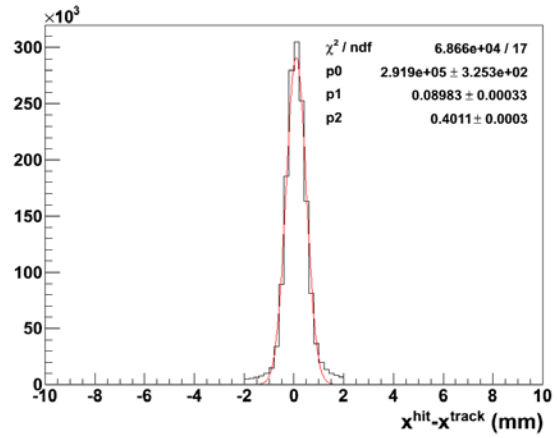

Figure 2: Residuals of hit timing (nsec) at H1 with respect to the projected timing from the track. The width of 0.40 nsec in r.m.s. is obtained.

Fig. 3 shows QDC amplitude at H0 as a function of time-of-flight (t^{hit}_2-t^{hit}_0). At the time-of-flight around 10.5 nsec and the amplitude around 450, a single clear peak is seen. The peak time-of-flight value corresponds to proton energy of about 72 MeV. The horizontal bands around 100 and around 450 are due to accidental wrong combinations between a H0 hit and a H2 hit. No electron peak with β=1 around 3.8 nsec is observed.

Fig. 4 compares time-of-flight distributions at different track angle acceptance. The signal peak is the highest at the lowest angle range. The energies at the peak are 72.49 MeV at 3.6°-5.0°, 114.7 MeV at 6.0°-7.0°, and 79.05 MeV at 9.0°-11.0°. These energies are consistent with simulated H^+ energies of 40-110 MeV. The observed energies have tendency of lower energy at a higher angle, which may be due to higher energy loss since the track passes through longer effective thickness of the beam duct.

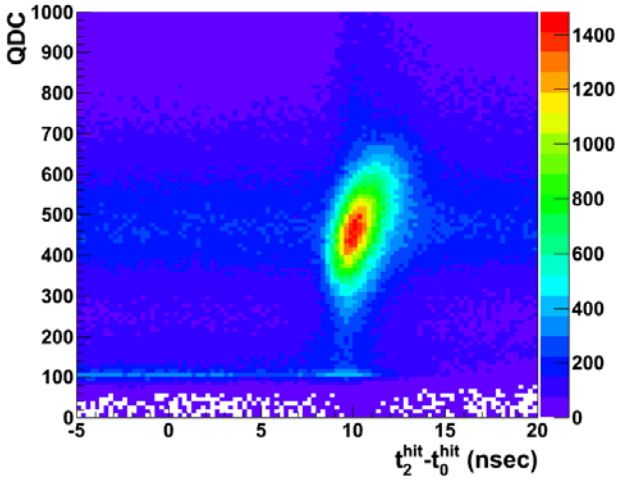

Figure 3: QDC amplitude (channel) at H0 as a function of time-of-flight (nsec) between H0 and H2 at 3.6.

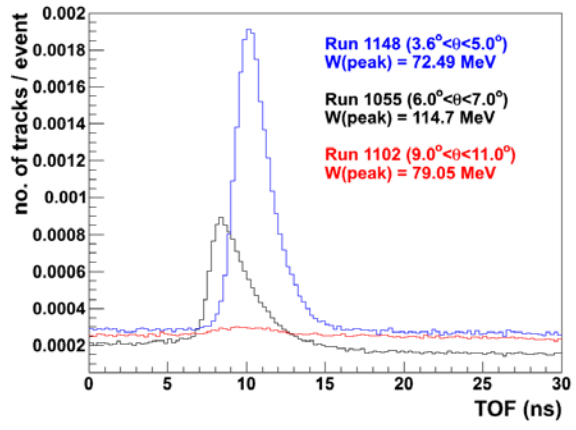

Figure 4: Time-of-flight (nsec) between H0 and H2 at the three geometry configurations.

Fig. 5 shows the projected z-position of each track to x=0, namely to the beam axis. The raw data (solid line) shows decreasing numbers of tracks toward upstream positions. However, as shown in Fig. 4, S/N is lower for downstream positions, and we estimated H^+ numbers from these distributions. The results are shown as dashed lines in Fig. 5. After the correction, the H^+ peak heights are similar at 6.0^o-7.0^o and 3.6^o-5.0^o, and corresponding z-ranges of 5400-6300 mm and 6900-9000 mm, while lower by the factor of 6 at 9.0^o-11.0^o and 4400-5000 mm.

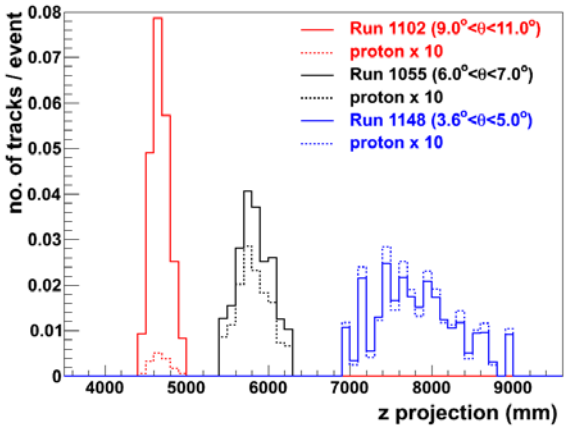

Figure 5: Projected-z positions of x-z tracks at three geometry configurations. Solid lines show raw numbers of tracks including accidental tracks, whereas the dashed lines are after the time-of-flight cuts and corrected to obtain proton numbers.

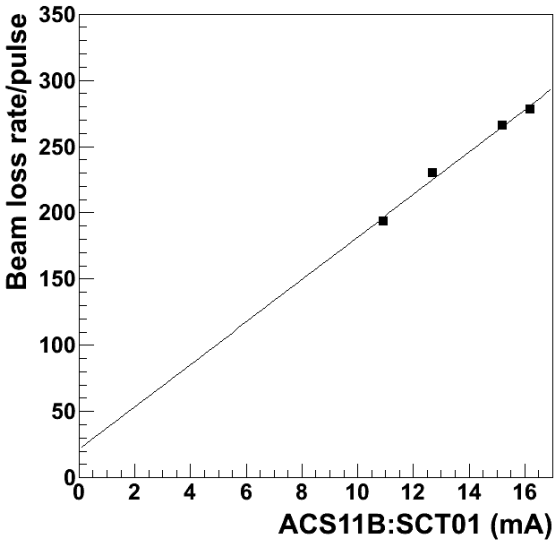

Figure 6: Beam loss rate per 100 μsec macro pulse with the trigger DY1&DY2&TG as a function of the peak beam current at a Slow Current Transformer (SCT) at the ACS section (mA).

We have examined linearlity of the trigger counts (DY1&DY3&TG) at TG width of 100 μsec with beam loss. We assume beam loss is proportional to the beam current, and measured bem loss rates and beam current while moving the beam stopper (scraper) position at upstream MEBT1 as shown in Fig. 6. The beam current is measured by a Slow Current Transformer at the ACS section. The line shows a straight line fit. The linearity is good, but a slight saturation seems to be observed at two points with high beam current. In this measurement, we used a special geometry configuration. The distance between H0/1 and H2/3 was set to be much shorter (a few 10 mm), and the horizontal distance to the beam duct was 785 mm. In the normal geometry for time-of-flight measurements, the beam loss rate per pulse (the y-axis in Fig. 6) is around 235.

CONCLUSIONS

A clear time-of-flight signal consistent with H^+ has been observed with the improved trigger method with PMT dynode signals. Assuming H^+, the energy is 72.5-114.7 MeV, which is cosistent with simulation. In the measured angle ranges, the H^+ rate is highest at the lowest angle ranges of 3.6^o-5.0^o. The beam loss distributions along the beam axis are demonstrated.

During summer shutdown period in 2012, we plan several detector upgrades for the next beam operation starting from Oct 2012. We are going to increase the number of fibers to read out for each plane and are currently constructing two fiber planes for vertical position measurements, which enables vertical track reconstruction. We will install a remotely controlled detector moving system in x- and y-positions. With these upgrades, we expect to improve beam loss distribution measurements significantly. We are also preparing detailed detector simulation in order to estimate detector acceptance for absolute beam loss rate estimation.

ACKNOWLEDGEMENT

We thank J-PARC linac monitor group for supports of detector installation and tests. This work was supported by JSPS KAKENHI Grant Numbers 23656063 and 24510134.

REFERENCES

[1] H. Sako, *et al.*, "Beam Loss Particle Tracking in J-PARC Linac," 8th Annual Meeting of Particle Accelerator Society in Japan, Tsukuba, Japan, p. 501 (2011).

[2] H. Sako, *et al.*, "Measurement of Beam Loss Tracks by Scintillating Fibers at J-PARC Linac," IPAC11, San Sebastian, Spain, 2011, p. 1251 (2011).